Selective Enhancement of the Uptake and Bioactivity of a TAT-conjugated Peptide Inhibitor of Glycogen Synthase Kinase-3

Aziza P Manceur[1,2], Brandon D Driscoll[1,2], Wei Sun[1,2] and Julie Audet[1,2]

[1]Institute of Biomaterials and Biomedical Engineering, University of Toronto, Toronto, Ontario, Canada; [2]Terrence Donnelly Centre for Cellular and Biomolecular Research, University of Toronto, Toronto, Ontario, Canada

The use of cell-penetrating peptides as transduction vectors is a promising approach to deliver peptides and proteins into cells. However, the uptake and bioavailability of trans-activating transcriptor (TAT)-conjugated molecules vary depending on the cell type and the cargo. This study aimed to determine whether a low-voltage electrical pulse can enhance the TAT-mediated delivery of peptide cargoes in different cell types. In TF-1 and mouse embryonic stem cells, the uptake of a novel detachable TAT-conjugated glycogen synthase kinase-3 (GSK-3) peptide inhibitor was enhanced by an order of magnitude without affecting the cell viability. A similar increase in uptake was achieved in primary mouse bone marrow cells while maintaining >80% of their viability. Interestingly, under these low-voltage conditions, the uptake of a control peptide not conjugated to TAT was not significantly increased. A T-cell factor/lymphoid enhancer factor (TCF/LEF) luciferase reporter assay was also used to assess the bioactivity of the TAT construct. The results indicated that cells loaded with a low-voltage electrical pulse had a two-fold increase in TCF/LEF activity, which was equivalent to a level of GSK-3 inhibition similar to that of cells treated with 20 mmol/l lithium or 500 nmol/l (2′*Z*,3′*E*)-6-bromoindirubin-3′-oxime. These results demonstrate the usefulness of low-voltage electrical pulses to enhance the uptake and bioactivity of TAT-conjugated molecules in different cell types.

Received 22 July 2008; accepted 10 November 2008; published online 23 December 2008. doi:10.1038/mt.2008.271

INTRODUCTION

Several recent studies have demonstrated the potential of trans-activating transcriptor (TAT)-mediated delivery of proteins and peptides in the development of clinical approaches, including therapeutic and prophylactic vaccines[1–3] and stem cell–based cellular therapies.[4–6] The most significant advantages of using cell-penetrating peptides such as TAT as transduction vectors is that they allow the transient engineering of cells without the need for viral vectors. The mechanism by which TAT can transport a variety of molecules in cells has not been completely elucidated. TAT-mediated transduction initially involves a strong ionic interaction between TAT and the cell membrane. The penetration steps that follow have been reported to rely on either energy-independent processes such as the formation of inverse micelles,[7] destabilization of the lipid bilayer and pore formation,[8] or active processes based on vesicular uptake and macropinocytosis.[9–11]

A major bottleneck in the optimization and widespread use of TAT-mediated delivery of peptides and proteins is that the efficiency of transduction depends on both the nature of the cargo[12] and the cell type.[13] For instance, some studies have suggested that differences in TAT uptake between cell types may be related to their respective amount of heparan sulfate proteoglycans present on the cell surface.[13–16] On the other hand, maximizing the uptake may not always be sufficient in a given application; the bioavailability and bioactivity of the construct also need to be controlled and optimized. To this end, different strategies have been employed such as endosomes disruption with chloroquine,[17] calcium,[18] sucrose,[19] and photosensitizers.[20] For instance, fusion of TAT to a peptide made of 20 amino acids isolated from the hemagglutinin protein of influenza virus was also found to improve endosomal escape.[21] In practice, however, some of these treatments can be associated with significant cell toxicity.

The objective of this study was to determine whether low-voltage electrical pulses can be used to enhance the intracellular uptake and bioactivity of peptide cargoes. A human hematopoietic progenitor cell line (TF-1), mouse R1 embryonic stem cells (R1 ESCs), and primary mouse bone marrow (BM) cells were transduced with a detachable TAT-conjugated glycogen synthase kinase-3 (GSK-3) substrate based on a peptide sequence derived from the eukaryotic initiation factor 2B (eIF2B). High levels of intracellular accumulation of the eIF2B peptide were achieved by combining TAT-mediated delivery with electrical pulses at voltages that are lower than those typically used for electroporation. The bioactivity of TAT-eIF2B in cells was evaluated from its ability to competitively inhibit the phosphorylation of β-catenin by GSK-3 and increase the T-cell factor/lymphoid enhancer factor (TCF/LEF) activity in a luciferase reporter assay.

Correspondence: *Julie Audet, Assistant Professor, 164 College Street, RS 407, Institute of Biomaterials and Biomedical Engineering, Terrence Donnelly Centre for Cellular and Biomolecular Research, University of Toronto, Toronto, Ontario M5S 3G9, Canada. E-mail: julie.audet@utoronto.ca*

RESULTS

Low-voltage electrical pulses selectively enhance the uptake of TAT constructs

TAT-eIF2B is composed of a 16 amino acid peptide sequence derived from eIF2B that was fluorescently labeled with 5-FAM and conjugated to TAT via two cysteines to form a detachable disulfide bond (**Table 1**). The cellular uptake of TAT-eIF2B was evaluated in TF-1 cells and compared to that of unconjugated TAT and eIF2B (**Figure 1a**). The uptake of each peptide was assessed from the fold change in median fluorescence intensity (MFI) relative to untreated cells.[13] The uptake of TAT-eIF2B was similar to that of TAT (3.7 ± 1.7-fold change in MFI versus 4.3 ± 0.7-fold change in MFI, respectively) and the uptake of eIF2B was negligible (1.8 ± 0.3-fold change in MFI compared with untreated cells). Next, TF-1 cells were exposed to electrical pulses of increasing intensities, in the presence of the same peptides (**Figure 1a**). The uptake of TAT increased from 10 ± 6- to 951 ± 4-fold change in MFI as the voltage was increased from 80 to 200 V. The uptake of TAT-eIF2B increased in the same manner, but its absolute value was on average ~50% of that obtained with TAT. Similar measurements were then obtained with R1 ESCs (**Figure 1b**) and primary BM cells (**Figure 1c**). From 0 to 200 V, the uptake of TAT in R1 ESC increased from 8 ± 2- to 450 ±110-fold change in MFI (**Figure 1b**). Higher voltages were required to achieve a significant increase in TAT-mediated uptake in primary BM cells. From 0 to 340 V, the uptake of TAT increased from 10 ± 3- to 555 ± 22-fold change in MFI, and the uptake of TAT-eIF2B increased in a similar fashion; however, its absolute value was on average ~50% of that obtained with TAT (**Figure 1c**). In all cell types, in the range of voltages tested, the uptake of eIF2B did not go significantly above tenfold change in MFI.

Enhancement of TAT-eIF2B uptake using electrical pulses can be performed without significant toxicity to the cells

Electroporation (the use of electrical pulses to permeabilize the cell membrane) is a common method for transfecting molecules into mammalian cells, but loss of cell viability is a significant drawback. Even though the electrical pulses used in these experiments were lower than those typically used for electroporation, it was not clear whether they would have a lesser impact on cell viability. A viability analysis of the cells was then performed to determine whether the increase in TAT and TAT-eIF2B uptake was associated with significant toxicity. For all cell types, the proportion of necrotic (PI^+) cells increased at higher voltages (**Supplementary Figure S1a–c**); this effect was more pronounced for R1 ESC (**Supplementary Figure S1b**). Because useful conditions for transduction require achieving a substantial increase in uptake with minimal cell toxicity, a statistical analysis of the uptake and viability data was performed and the voltage that corresponds to the maximum increase in uptake without significant reduction in cell viability was identified. The results presented in **Table 2** illustrate clearly the potential usefulness of this approach for, specifically, TAT-conjugated molecules, as opposed to Antennapedia (Antp) constructs or unconjugated peptides. For instance, using a 120–130 V pulse, the uptake of TAT and TAT-eIF2B was increased by >20-fold relative to 0 V, without significantly affecting the

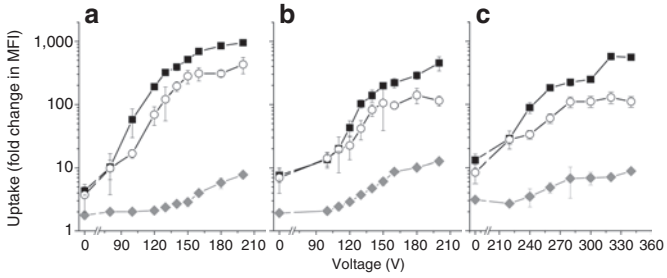

Figure 1 Low-voltage electrical pulses significantly enhance trans-activating transcriptor (TAT)-mediated uptake in different cell types. Uptake of TAT (squares), TAT-eIF2B (circles), or eIF2B (diamonds) in (**a**) TF-1 cells, (**b**) R1 embryonic stem cells (R1 ESCs), and (**c**) bone marrow (BM) cells. Fluorescently labeled peptides were added at 10 µmol/l to 10^5 cells kept on ice in 100 µl Hanks balanced salt solution (HBSS) without calcium or magnesium. Cells in cold HBSS were then immediately exposed to a single electrical pulse of a specific voltage in cuvettes with an electrode gap of 2 mm, using a capacitance of 500 µF and a pulse duration of 1.5–2.0 ms. Cells that were not exposed to an electrical pulse were incubated with peptides on ice at the same time. Cells in both groups were then thoroughly washed to remove cell surface–bound peptides, and the mean fluorescence intensity (MFI) of the cell sample was measured by flow cytometry. The uptake was expressed as fold change in MFI (±SD, $n = 3$) relative to a cell sample in which fluorescently labeled peptides were not added. eIF2B, eukaryotic initiation factor 2B.

Table 1 Construct sequences, molecular weights, and isoelectric points

Construct	Sequence[a–e]	Molecular weight (kd)	Isoelectric point[f]
TAT	5-FAM-CYGRKKRRQRRR-NH_2	1.7	12.7
Antp[g]	FITC-LC-RQIKIWFQNRRMKWKK-NH_2	2.2	14.0
eIF2B	5-FAM-RRAAEELDSRAGS(p)PQL-NH_2	1.8	8.3
TAT-eIF2B	5-FAM-RRAAEELDSRAGS(p)PQLC-(S-S)-CYGRKKRRQRRR-NH_2	3.5	12.1
TAT-eIF2BΔRR	5-FAM-AAEELDSRAGS(p)PQLC-(S-S)-CYGRKKRRQRRR-NH_2	3.2	11.7
Antp-eIF2B[g]	5-FAM-RRAAEELDSRAGS(p)PQLC-(S-S)-CRQIKIWFQNRRMKWKK-NH_2	4.2	11.8
TAT-pepA	5-FAM-KVLTQMGSPSIRCSS(p)VAC-(S-S)-CYGRKKRRQRRR-NH_2	3.5	12.3
TAT-pepS	5-FAM-KVLTQMGSPSIRCSS(p)VSC-(S-S)-CYGRKKRRQRRR-NH_2	3.5	12.3
TAT-SA-PE	$(TAT\text{-}biotin)_x$-(SA-PE)[h]	300[f]	4–5

Abbreviations: eIF2B, eukaryotic initiation factor 2B; TAT, trans-activating transcriptor.
[a]5-FAM denotes carboxyfluorescein. [b]FITC denotes fluorescein isothiocyanate. [c]LC denotes a 6-aminohexanoic acid linker. [d]S(p) denotes a phosphoserine. [e]-(S-S)- denotes a disulfide bond linkage. [f]Molecular weight for a complex with $x = 4$. The isoelectric point do not take into account 5-FAM or FITC. [f]Antp denotes Antennapedia. [g]The maximal theoretical valency (x) is 4 but the molar ratio of TAT-biotin to streptavidin-phycoerythrin (SA-PE) used in the experiment allows a x value between 3 and 4.

Table 2 Enhancement of trans-activating transcriptor (TAT)-mediated uptake using low-voltage electrical pulses

Cell type	Peptide	Increase in uptake relative to 0 V (fold ± SD)	Voltage (V)	Viability[a] (%)
TF-1	TAT	44 ± 8	120[b]	83 ± 2
	TAT-eIF2B	27 ± 7	130[b]	78 ± 7
	Antp	6 ± 1	130[b]	76 ± 1
	Antp-eIF2B	5 ± 3	130[b]	76 ± 10
	eIF2B	4 ± 1	200[b]	77 ± 18
R1 ESC	TAT	14 ± 4	130[b]	75 ± 5
	TAT-eIF2B	6 ± 3	130[b]	71 ± 3
	Antp	4 ± 1	140[b]	73 ± 5
	Antp-eIF2B	2.0 ± 0.4	140[b]	78 ± 2
	eIF2B	2.0 ± 0.2	130[b]	85 ± 4
BM	TAT	16 ± 5	260[c]	84 ± 2
	TAT-eIF2B	7 ± 3	260[c]	81 ± 6
	Antp	6 ± 1	260[c]	79 ± 4
	Antp-eIF2B	6 ± 2	260[c]	82 ± 7
	eIF2B	3 ± 2	280[c]	87 ± 3

Abbreviations: Antp, Antennapedia; BM, bone marrow; eIF2B, eukaryotic initiation factor 2B; R1 ESC, R1 embryonic stem cell.
[a]Cell viability was evaluated from the number of propidium iodide positive (PI^+) cells measured by flow cytometry; a conservative gating strategy was used and the events recorded did not exclude cell debris in the treated cell samples. The data are expressed as mean ± SD ($n = 3$). [b]Voltage at which a maximum enhancement of TAT-mediated uptake was achieved without a significant change in viability. This data were obtained by performing an ANOVA test ($\alpha = 0.05$) on the results presented in **Figure 1** and **Supplementary Figure S1**. [c]Voltage at which a maximum enhancement of uptake was achieved while the viability remained above 80%.

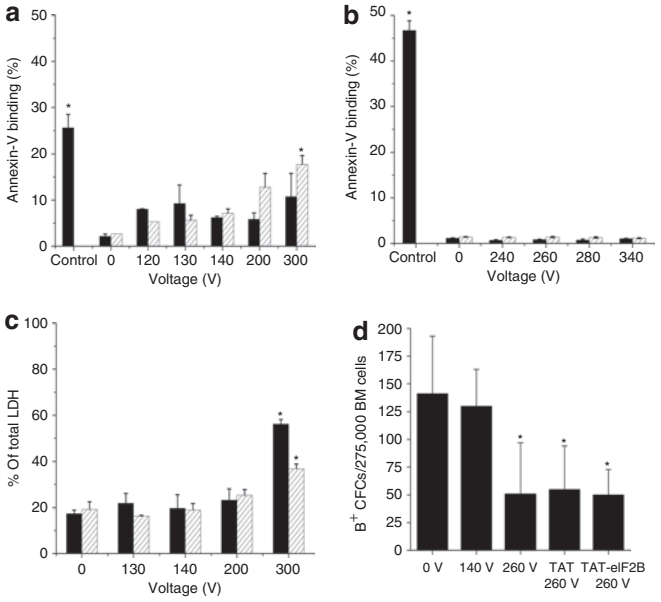

Figure 2 Low-voltage electrical pulses have minimal cell toxicity. Cells were exposed to an electrical pulse of a specific voltage in the absence (filled bars) or presence (hatched bars) of trans-activating transcriptor (TAT), as described in **Figure 1**. Annexin-V binding (Annexin-V^+ cells in the 7-amino-actinomycin D^- subset) was measured by flow cytometry for (**a**) TF-1 cells (mean ± SD, $n = 2$) and (**b**) bone marrow (BM) cells (mean ± SD, $n = 2$). The positive control consisted of cells treated with the cytotoxic agent camptothecin for 6 hours at a concentration of 50 nmol/l. (**c**) Membrane leakage was measured by lactate dehydrogenase (LDH) release from TF-1 cells (mean ± SD, $n = 2$). Total (100%) LDH release was defined with a sample of cells lysed in cell lysis buffer. (**d**) BM erythroid progenitor cells (B^+ CFCs) were assayed with a colony-forming cell (CFC) assay by plating 25,000 BM cells per ml of methylcellulose medium supplemented with cytokines. After 7 days, the colonies containing hemoglobin were stained with benzidine and scored (mean ± SD, $n = 4$). eIF2B, eukaryotic initiation factor 2B. Asterisk denotes that the difference is significant at $\alpha = 0.05$ (ANOVA *t*-test).

viability of TF-1 cells; the increase for Antp and Antp-eIF2B at 130 V was significantly lower (approximately fivefold increase in uptake relative to 0 V). For R1 ESC, the maximum increase in TAT and TAT-eIF2B uptake achievable without significant loss of viability was also found at 130 V. At this voltage, the increase in uptake relative to 0 V was more than fivefold, which is significant but much lower than for TF-1. The increase in uptake in R1 ESC for Antp and Antp-eIF2B at 140 V was less than fivefold (relative to 0 V), which is significantly lower than for TAT and TAT-eIF2B. With BM cells, it was not possible to identify a voltage at which cell viability was not significantly decreased. However, the cell viability remained above 80% at 260 V (**Supplementary Figure S1c**); these conditions resulted in an increase in TAT and TAT-eIF2B uptake of more than sevenfold relative to 0 V. The increase in uptake for Antp and Antp-eIF2B at 260 V in BM was less than sevenfold relative to 0 V.

An Annexin-V binding assay and a lactate dehydrogenase (LDH) leakage assay were also used to assess, respectively, apoptosis and loss of membrane integrity. In TF-1 cells, the effect of electrical pulses on Annexin-V binding were not significant, up to a voltage of 200 V (**Figure 2a**); for BM cells, no significant increase in apoptotic (Annexin-V^+) cells was observed up to 340 V (**Figure 2b**). LDH leakage in TF-1 cells did not show any significant increase up to 300 V (**Figure 2c**). The effect of electrical pulses on Annexin-V binding and LDH leakage in TF-1 cells were significantly higher in the presence of TAT but only at voltages ≥ 200 and 300 V, respectively (**Figure 2a,c**). To assess toxicity in a more stringent fashion, the change in the number of erythroid progenitor cells in the BM sample was determined using a colony-forming cell (CFC) assay[22] combined with a hemoglobin stain using benzidine (B^+) (**Figure 2d**). BM cells treated with a 140 V electrical pulse did not have a reduced number of B^+ CFCs (erythroid colonies) compared with untreated (0 V) cells, and BM cells exposed to 260 V gave rise to ~50% fewer colonies. TAT or TAT-eIF2B did not have any significant effect on the number of B^+ CFCs.

To determine whether the levels of uptake obtained using electrical pulses could be reached by simply increasing the TAT-construct concentration, the uptake of TAT-eIF2B in TF-1 cells loaded at 5, 10, 25, and 50 µmol/l was measured at 0 V and compared to that obtained at 130 V (**Figure 3a**). As expected, at any peptide concentrations, the electrical pulse significantly increased the uptake. However, the uptake measured with 50 µmol/l TAT-eIF2B at 0 V was almost three times lower than that obtained with 10 µmol/l TAT-eIF2B at 130 V (28 ± 1-fold change in MFI versus 80 ± 1-fold change in MFI, respectively). Moreover, higher concentrations (25 and 50 µmol/l) were associated with significant loss of viability, even in cells loaded without an electrical pulse

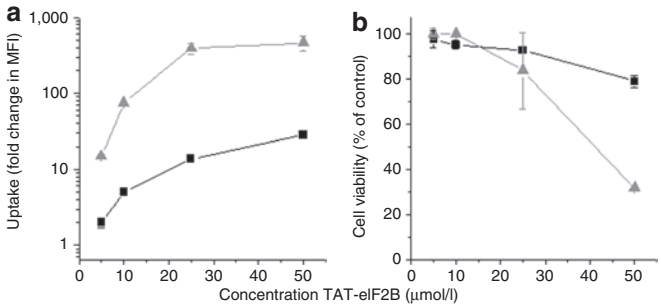

Figure 3 Higher TAT-eIF2B concentrations cannot substitute for the electrical pulse treatment in enhancing the trans-activating transcriptor (TAT)-mediated uptake. (**a**) Uptake in TF-1 cells measured with increasing concentrations of TAT-eIF2B at 0 (squares) or 130 V (Triangles). The uptake was measured in viable (PI^-) cells. (**b**) TF-1 cell viability following exposure to increasing concentrations of TAT-eIF2B at 0 (squares) and 130 V (Triangles). The cells were loaded with peptides as described in **Figure 1**. The viability is measured with a propidium iodide (PI) stain by flow cytometry and is expressed relative to the number of viable (PI^-) cells in the untreated control-cell sample. In all panels, data are expressed as mean ± SD (n = 3). eIF2B, eukaryotic initiation factor 2B.

(**Figure 3b**); the cell viability with 50 μmol/l TAT-eIF2B at 0 V was ~20% lower than that obtained with 10 μmol/l TAT-eIF2B at 130 V. Thus, in TF-1 cells, the results confirmed that 10 μmol/l TAT-eIF2B at 130 V maximized the uptake and viability.

Electrical pulses can improve the transduction of constructs that have initially either a high or low uptake

TAT-eIF2B had initially a relatively low cell permeability at 0 V (less than tenfold change in MFI at 0 V, **Figure 1**), and the uptake was significantly increased with a low-voltage pulse for all cell types. However, it was still unclear whether this substantial enhancement in uptake was a phenomenon restricted to this particular construct or whether this approach could be useful to improve the transduction of other TAT-conjugated cargoes that have initially lower or higher levels of uptake. A TAT-conjugated peptide with a slightly lower uptake than TAT-eIF2B (**Figure 4a**) was created by removing two arginines at the N terminus of the eIF2B peptide cargo (eIF2B-ΔRR). At 130 V, the uptake of TAT-eIF2B-ΔRR in TF-1 cells still increased significantly (17 ± 6-fold relative to 0 V, **Figure 4a**). Next, the uptake of another construct, TAT-pepS, was measured at 0 and 130 V. TAT-pepS is similar to TAT-eIF2B in that it is composed of a peptide derived from the protein Smad3[23] (a serine/threonine kinase substrate) that has been conjugated to TAT via two cysteines to form a detachable disulfide bond (**Table 1**); however, TAT-pepS has a much higher uptake at 0 V (~ 100-fold change in MFI, **Figure 4a**). The uptake of TAT-pepS increased as well in cells loaded with an electrical pulse but only by 2.8 ± 0.3-fold relative to 0 V (**Figure 4a**). One serine residue (polar uncharged, hydrophilic) in TAT-pepS was substituted for one alanine residue (polar uncharged, hydrophobic). The resulting construct was designated as TAT-pepA (**Table 1**). TAT-pepS and TAT-pepA do not significantly differ in molecular weight or charge, but the uptake measurements showed that this minor substitution was sufficient to significantly decrease the uptake at both 0 and 130 V (**Figure 4a**). As

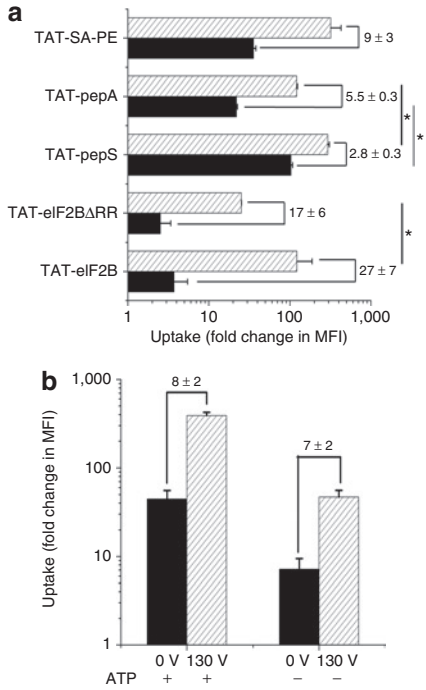

Figure 4 An electrical pulse can enhance the uptake of a variety of trans-activating transcriptor (TAT)-conjugated cargoes and in adenosine triphosphate (ATP)-depleted cells. (**a**) Uptake of TAT-eIF2B, TAT-eIF2BΔRR, TAT-pepS, TAT-pepA, TAT-SA-PE at 0 (filled bars), and 130 V (hatched bars) in TF-1 cells (mean ± SD, n =3). TAT-eIF2BΔRR is composed of an eukaryotic initiation factor 2B (eIF2B) peptide truncated of two arginines. TAT-pepS and TAT-pepA differ by only one amino acid residue substitution (serine → alanine). TAT-SA-PE is TAT-biotin complexed with a fluorescent fusion protein streptavidin-phycoerythrin (SA-PE); the complex was prepared by combining TAT-biotin with SA-PE at 10 and 3 μmol/l, respectively. The mixture was preincubated on ice for 20 minutes in 100 μl Hanks balanced salt solution without calcium or magnesium. The cells were loaded with peptides and proteins as in **Figure 1**. The numbers above the bars indicate the amount of (±SD) increase in mean fluorescence intensity (MFI) from 0 to 130 V. Asterisk denotes that the difference is significant at α = 0.05 (ANOVA test). (**b**) TAT uptake in TF-1 cells depleted of ATP or under normal conditions (mean ± SD, n = 2). TF-1 cells were exposed to 10 μmol/l TAT and were treated at 0 or 130 V. ATP depletion was performed before adding peptides and was achieved by incubating cells in 10 mmol/l sodium azide and 6 mmol/l 2-deoxy-D-glucose in Hanks balanced salt solution without calcium or magnesium for 1 hour at 37 °C. The numbers above the bars indicate the amount of (±SD) increase in MFI from 0 to 130 V.

expected, the fold enhancement in uptake relative to 0 V for TAT-pepA was higher than for TAT-pepS (5.5 ± 0.3-fold versus 2.8 ± 0.3-fold, **Figure 4a**). Finally, streptavidin-phycoerythrin (SA-PE) was tested as a model protein cargo to determine whether a low-voltage electrical pulse can also enhance the uptake of proteins. In this experiment, TAT-biotin was mixed with SA-PE and added to TF-1 cells that were next exposed to a 130 V electrical pulse. Significant enhancement of the uptake of the TAT-SA-PE complex was also observed in cells treated with an electrical pulse (**Figure 4a**). The increase in the uptake at 130 V was substantial (9 ± 3-fold relative to 0 V) and was greater than for TAT-pepS and TAT-pepA but lower than for TAT-eIF2B and TAT-eIF2B-ΔRR. The MFI of TAT-SA-PE was much higher than TAT-eIF2B (**Figure 4a**). This is due to the brightness of PE which is much greater than that of fluorescein (up to 20-fold).[24] Moreover, each

SA-PE molecule can be bound to multiple TAT-biotin molecules (**Table 1**) which can contribute to increasing the uptake.[25]

To provide some insights into the mechanisms by which a low-voltage electrical pulse enhances the TAT-mediated uptake of various cargoes, the loading procedure was modified. First, adenosine triphosphate (ATP) was depleted from TF-1 cells before exposing them to a 130 V electrical pulse in the presence of TAT (**Figure 4b**). The uptake of TAT was in part, but not completely, energy-dependent because depleting cells of ATP resulted in 80% decrease in the uptake at both 0 and 130 V. Consequently, the increase in uptake observed at 130 V was similar in both conditions (7 ± 2-fold increase relative to 0 V in normal conditions versus 8 ± 2-fold increase relative to 0 V in ATP-depleted conditions). The results clearly showed that an electrical pulse can substantially increase the uptake even in ATP-depleted conditions; however, maximization of the intracellular uptake using this approach requires ATP.

Although the uptake of both TAT-SA-PE and TAT-eIF2B could be enhanced using electrical pulses, confocal images revealed that the subcellular distribution of the peptide and the protein were different (**Figure 5a–d**). The fluorescence of TF-1 cells loaded with TAT-SA-PE at 0 (**Figure 5a**) and 140 V (**Figure 5b**) appeared punctuated and mainly excluded from the nucleus (see **Supplementary Figure S2** for the composite images with the nuclear stain), while the fluorescence of cells loaded with TAT-eIF2B was homogeneously distributed throughout the cell at both 0 (**Figure 5c**) and 130 V (**Figure 5d**). A similar homogenous intracellular distribution was observed for TAT-pepA and TAT-pepS as well (data not shown).

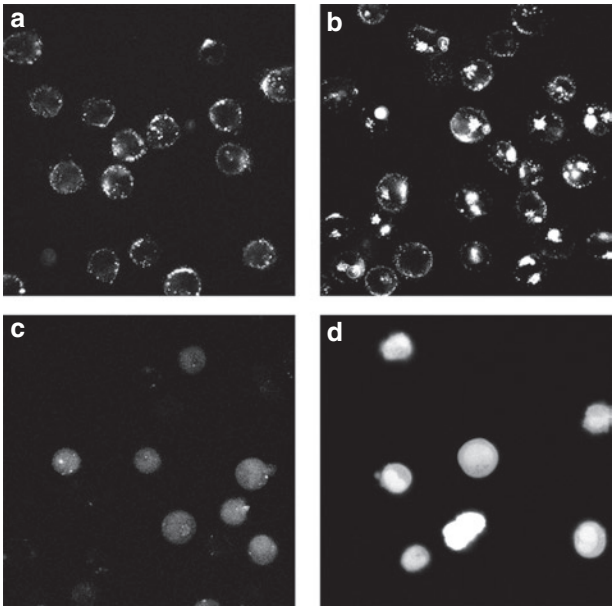

Figure 5 The intracellular localization of the eukaryotic initiation factor 2B (eIF2B) peptide cargo is different than that of the streptavidin-phycoerythrin (SA-PE) protein cargo. Confocal microscopy images of TF-1 cells treated with TAT-SA-PE at (**a**) 0 and (**b**) 140 V, and TF-1 cells exposed to TAT-eIF2B at (**c**) 0 and (**d**) 130 V. SA-PE denotes streptavidin-phycoerythrin and TAT-SA-PE is trans-activating transcriptor (TAT)-biotin complexed with SA-PE. Composite color images are presented in **Supplementary Figure S2**. The cells were loaded with peptides and proteins as described in **Figure 1**. Cells were kept on ice. Images were taken 30–60 minutes after loading.

TAT-eIF2B internalized in cells is bioactive and can act as a competitive inhibitor of GSK-3

The eIF2B peptide used in this study is a GSK-3 substrate.[26] A detachable, reducible disulfide bond formed a cleavage site between TAT and the substrate peptide (**Table 1**); the purpose of this cleavage site was to prevent TAT from decreasing the bioactivity of the eIF2B peptide by influencing its intracellular distribution or by hindering its interaction with GSK-3.[27] At high concentrations, eIF2B can competitively inhibit the phosphorylation of β-catenin[28] and can increase the accumulation of β-catenin and its interaction with members of the TCF/LEF family of transcription factors. To determine whether the increase in TAT-eIF2B uptake produced by a low-voltage electrical pulse resulted in an increase in the intracellular activity of eIF2B, TF-1 cells were transfected with a TCF/LEF luciferase reporter gene. Next, these cells were pulsed at 140 V in the presence of TAT-eIF2B, TAT, or eIF2B, and then the luciferase signals were compared with those of cells treated with TAT-eIF2B, TAT, or eIF2B at 0 V (**Figure 6**). The bioactivity results were in agreement with the uptake measurements obtained previously, and TCF activity was higher in cells treated with TAT-eIF2B at 140 V (twofold increase in luciferase signal relative to TAT-eIF2B loaded at 0 V). Moreover, the level of TCF activity measured with TAT-eIF2B at 140 V was not significantly different than that obtained with the GSK-3 inhibitors lithium (LiCl) and (2′*Z*,3′*E*)-6-Bromoindirubin-3′-oxime (BIO) (used at 20 mmol/l and 500 nmol/l, respectively).

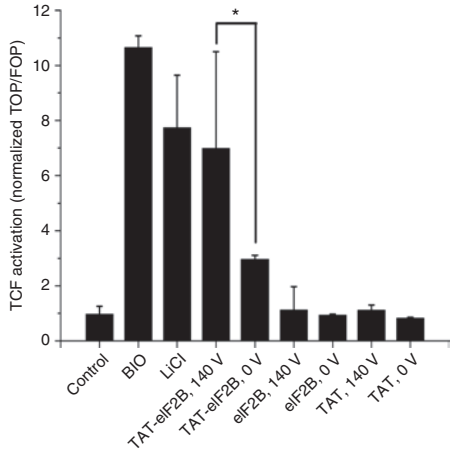

Figure 6 Increased bioactivity of TAT-eIF2B in cells loaded using a low-voltage electrical pulse. TF-1 cells were transfected with the reporter gene TOP-5 harboring T-cell factor/lymphoid enhancer factor (TCF/LEF) binding sites for β-catenin and the corresponding FOP-5 without these sites as a control. Cells were incubated with either 500 nmol/l (2′*Z*,3′*E*)-6-bromoindirubin-3′-oxime (BIO) or 20 mmol/l lithium (LiCl); or with 10 μmol/l TAT-eIF2B, trans-activating transcriptor (TAT), or eukaryotic initiation factor 2B (eIF2B) for 24 hours; or exposed to a 140 V electrical pulse in the presence of 10 μmol/l TAT-eIF2B, TAT, or eIF2B; and then incubated for 24 hours. TCF activity is expressed as the ratio of TOP-5/FOP-5 (mean ± SD, $n = 3$). Asterisk denotes that the difference is significant at $\alpha = 0.05$ (ANOVA test).

DISCUSSION

TAT-mediated delivery is a powerful approach for cell engineering. However, useful levels of uptake and activity can be difficult to achieve depending on the cargo and the cell type targeted. This study demonstrates that the delivery of TAT-conjugated peptides and proteins in cells can be significantly enhanced by using electrical pulses at voltages that are sufficiently low to maintain cell viability and minimize toxicity. The optimal voltages are also dependent on the cell type, but are always below the values conventionally used for electroporation. For instance, the transfection of TF-1 cells is usually performed with voltages ranging from 240 to 350 V,[29,30] and this study shows that an optimal voltage of 130–140 V enhanced the uptake of TAT-eIF2B by an order of magnitude without observable toxicity. The increase in the uptake of TAT-eIF2B in cells translated into a greater than twofold increase in the bioactivity of the cargo compared with cells that had not been loaded with an electrical pulse. This enhancement was sufficient to maximize the intracellular activity of eIF2B and attain levels of TCF activation similar to that obtained with saturating concentrations of two pharmacological inhibitors, either lithium or BIO. The optimal voltage identified for R1 ESC was also in the same range (130 V), and those cells are commonly transfected with electroporation voltages ranging from 230 to 800 V.[31] Due to their smaller diameter, primary BM cells are usually electroporated at higher voltages than TF-1 or R1 ESC, typically around 300–320 V.[32–34] TAT-mediated uptake in BM cells was significantly enhanced at 260 V. At this voltage, the viability of the BM cells remained high (>80%) and approximately half the erythroid progenitor colony-forming activity was preserved.

For all cell types investigated, it was possible to identify a range of voltages where the uptake of only TAT or TAT-conjugated peptides was increased. This suggests that these low voltages alone are not sufficient to create pores in the cell membrane. The uptake of TAT, either in the absence or presence of an electrical pulse, was decreased in ATP-depleted cells. However, exposure to an electrical pulse can significantly enhance the uptake in spite of ATP depletion. This suggests that the enhancement of TAT-mediated transduction with an electrical pulse depends on the cooperation between energy-dependent and independent mechanisms. For instance, the electric pulse may increase the adsorption of TAT constructs (peptides and proteins) on the cell surface. Subsequently, internalization would proceed as in normal conditions (0 V), via endosomal uptake and other possible transduction mechanisms. These subsequent mechanisms may differ for proteins or peptides. Antov *et al.* studied the uptake of albumin in cells exposed for 1 minute to a train of very low-voltage electrical pulses.[35,36] They first observed an increased adsorption of albumin on the cell surface. They proposed a series of possible phenomena to explain the transient change in the adsorptive properties of the cell surface; one that may apply to this study (cells exposed to a single 2-ms pulse of 650 V/cm) is the induction of the electrophoretic segregation of charged components at the cell surface;[36] it is plausible that selectively facilitated the adsorption of TAT and TAT constructs on this membrane. Antov *et al.*[36] reported a second effect of the electrical pulses that can result in an enhancement of cellular uptake. They observed increased endosomal uptake of albumin following exposure to the train of pulses and increased vesicle formation and fusion "which resulted in massively patched fluorescent patterns in the cytosol (…)." As expected, this second mechanism was shown to be energy dependent. It is possible that this mechanism also plays a significant role in the uptake of TAT-SA-PE because the intracellular distribution of their protein appears to be similar to that presented here with TAT-SA-PE (**Figure 5a,b**). Interestingly, the electrical pulse was significantly less effective for enhancing Antp-mediated transduction, which is probably the consequence of the distinct mechanisms of membrane penetration[37] or a lowest affinity of Antp for the cell membrane compared with TAT after exposure to an electrical pulse.

This study demonstrates the usefulness of low-voltage electrical pulses to increase the uptake of TAT-conjugated peptides that have initially either a low (fivefold change in MFI at 0 V) or a high (100-fold change in MFI at 0 V) transduction efficiency. Moreover, the results suggest that this approach is also applicable to proteins. On the other hand, the bioavailability and bioactivity of the proteins and larger cargoes delivered in this manner still raise some concerns. TAT-SA-PE (*i.e.*, cargo size of 293 kd) loaded in TF-1 cells with and without electric pulses was present as large intracellular aggregates or in vesicles, while TAT-eIF2B (*i.e.*, cargo size of 2 kd) was diffuse and generally homogeneously distributed in the cells. Moreover, unlike TAT-eIF2B, TAT-SA-PE was excluded from the nucleus. These observations are consistent with the model proposed by Tunnemann *et al.* in which the size of the cargo attached to TAT determines the mode of entry in cells and intracellular trafficking; large constructs such as TAT-conjugated quantum dots and proteins are mainly endocytosed and remain largely trapped in cytoplasmic vesicles. The apparent bioactivity of the protein internalized in such manner represents the effect of a small fraction that escaped the endocytic compartments. The case is different for peptides that may be predominantly introduced in cells by membrane transduction and may have a greater bioactivity.[9] It is also possible that the differences observed in the subcellular distribution of the protein compared with the peptide cargoes are related to the different way they were conjugated to TAT. Interestingly, for both TAT-eIF2B and the TAT-SA-PE, confocal microscopy observations did not reveal any significant changes in the subcellular distribution of the cargo in cells loaded with an electrical pulse compared with those that were not. Because the use of low-voltage electrical pulses does not appear to modify the subcellular localization of the TAT-conjugated cargo, it has the potential to be useful for the delivery of TAT-conjugated protein only if the increase in uptake translates into a significant, greater amount of proteins leaking out of endocytic compartments.

In summary, this report demonstrates that low-voltage electrical pulses can be used to enhance the delivery of TAT-conjugated peptides and proteins in hematopoietic and embryonic cell lines as well as primary BM cells. Enhancement of the uptake by an order of magnitude can be obtained while maintaining a high yield and recovery of transduced cells. More importantly, the enhanced uptake can directly translate into a substantial increase in bioactivity of the cargo. Consequently, this approach can significantly facilitate functional studies of gene products and the development of novel molecular therapies based on nonviral vectors.

MATERIALS AND METHODS

Peptide synthesis. The peptide constructs used in this study are listed in **Table 1** along with their sequences. They were all custom-synthesized or

directly purchased from AnaSpec (San Jose, CA). SA-PE and biotin-TAT were also purchased from AnaSpec (San Jose, CA).

Cell isolation and cell culture. Animal tissues used in this study were obtained following standard procedures approved by the animal care committee of the University of Toronto. Mouse BM cells were flushed from the femurs and tibias of normal C57BL/6 adult mice into phosphate-buffered saline (PBS) containing 2% fetal bovine serum (FBS), as described in Miller *et al.*[38] Red blood cells were lysed in an ammonium chloride solution (Stem Cell Technologies, Vancouver, British Columbia, Canada). TF-1 cells (CRL-2003; American Type Culture Collection, Manassas, VA, USA), a factor-dependent human erythroleukemia cell line, were maintained in suspension cultures in T-flasks, in Roswell Park Memorial Institute (RPMI) 1640 medium (Gibco Invitrogen, San Diego, CA) supplemented with 10% FBS and 5 ng/ ml human granulocyte macrophage–colony-stimulating factor (R&D Systems, Minneapolis, MN). Mouse R1 ESCs were grown on gelatine-coated T-flasks in high-glucose Dulbecco's modified Eagle's medium supplemented with 0.1 mmol/l nonessential amino acids (Gibco Invitrogen, San Diego, CA), 1 mmol/l sodium pyruvate (Gibco Invitrogen, San Diego, CA), 100 μmol/l β-mercaptoethanol (Sigma, St. Louis, MO), 15% FBS, penicillin and streptomycin (final concentration 50 μg/ml each), and 1,000 U/ml leukemia inhibitory factor.[39] R1 ESC between passages 20 and 30 were used for these experiments.

Cell loading and treatment with electrical pulses. In this activity, 10^5 cells were resuspended in 100 μl Hanks balanced salt solution without calcium and magnesium and incubated on ice. After 15 minutes, fluorescently labeled peptides were added to a concentration of 10 μmol/l and cells were transferred into prechilled cuvettes with an electrode gap of 2 mm (E-Shot; Invitrogen, San Diego, CA). Control cells that were not treated with an electrical pulse were left on ice for 8–10 minutes (as described in Manceur *et al.*[13]), and the pulsed cells were immediately exposed to the desired voltage using a capacitance of 500 μF and a time constant/pulse duration between 1.5 and 2.0 ms. The electrical fields were generated using a Gene Pulser II (Bio-Rad, Hercules, CA). Immediately following the electrical pulse treatment, 400 μl of prewarmed Dulbecco's modified Eagle's media were added to the cells and control samples in a dropwise fashion that was followed by a 3-minute incubation at 37 °C. Cells were then gently transferred into Eppendorff tubes, centrifuged and resuspended in 100 μl prewarmed trypsin (1 mg/ml) at 37 °C for 10 minutes to remove surface-bound peptides. Trypsin was then neutralized by the addition of 300 μl of a solution of ice-cold phosphate-buffered saline containing 10% FBS and 1 μg/ml of the viability dye propidium iodide (PI). Cells were spun down and resuspended in 200 μl phosphate-buffered saline +2% FBS and analyzed with flow cytometry. In some experiments, cells were depleted from cellular ATP before adding peptides. This was achieved by incubating cells in ATP depletion buffer (10 mmol/l sodium azide and 6 mmol/l 2-deoxy-D-glucose in Hanks balanced salt solution without calcium and magnesium) for 1 hour at 37 °C[40] before loading.

Measurement of cellular uptake. Cellular uptake was measured as described in Manceur *et al.*[13] Peptide and protein uptake was measured using flow cytometry with a FACS Canto (BD Biosciences, San Jose, CA). The results were expressed as fold change in the MFI of the sample relative to a control sample not exposed to fluorescent peptides (change in MFI ± SD). The complete removal of fluorescent peptides on the cell surface was verified using trypan blue quenching, as described previously.[13]

Annexin-V binding assay. Annexin-V binding was evaluated by staining cells with PE-conjugated Annexin-V (Biovision, Mountain View, CA) in combination with the viability stain 7-amino-actinomycin D (Invitrogen, San Diego, CA) for exclusion of necrotic cells. Cells were incubated with Annexin-V-PE and 7-amino-actinomycin D at room temperature for 5 minutes in the dark, according to the manufacturer's instructions. The Annexin-V-PE signal was measured using flow cytometry on a FACSCanto (BD Biosciences, San Jose, CA).

LDH leakage assay. Membrane integrity was assessed by measuring the amount of LDH released by cells using the CytoTox-ONE assay (Promega, Madison, WI) according to the manufacturer instructions. In brief, 1×10^5 test cells and control-cell samples were incubated for 10 minutes with CytoTox-ONE reagent followed by stop solution. Fluorescence was measured at 560/590 nm in a multiwell plate reader. A 100% LDH release was obtained using cells lysed in cell lysis buffer (1% NP-40, 10 mmol/l Tris–HCl, 150 mmol/l NaCl, 5 mmol/l EDTA, 50 mmol/l NaF).

Erythroid CFC assay. CFC assays[38] were performed on samples of BM cells that had been exposed to low-voltage electrical pulses and on control samples. Aliquots of BM cells (27,500 per 35-mm Greiner dish) were plated in duplicate, and in 1.1 ml of semisolid culture medium (0.9% methylcellulose, 30% FBS, 1% bovine serum albumin, 10^{-4} mol/l β-mercaptoethanol) supplemented with 10 ng/ml mouse interleukin-3, 10 ng/ml human interleukin-6, 50 ng/ml mouse Stem Cell Factor, and 3 U/ml erythropoietin (MethoCult M3434; Stem Cell Technologies, Vancouver, British Columbia, Canada), according to the manufacturer's protocol. After a 7-day incubation at 37 °C, hemoglobinized colonies were detected by staining the cells with benzidine (Sigma, St. Louis, MO). Only the colonies containing at least 50 cells were scored.

Confocal microscopy. For imaging, cells were loaded with fluorescently labeled peptides as described above. Hoechst was added to stain the nucleus at a concentration of 1 μg/ml for 15 minutes on ice and PI (1 μg/ ml) was used to stain nonviable cells. Cell fluorescence was imaged on a Zeiss LSM510 confocal microscope (×63 objective) using poly-L-lysine-coated glass-bottom culture dishes (MatTek, Ashland, MA). Pictures were taken approximately at the center (*z*-direction) of the cells. The 5-FAM, Hoechst, and PI were excited using the 488, 364, and 543 nm laser lines, respectively. The 5-FAM signal was sorted out using a BP505-530 filter, the PE signal with a BP560-615 filter, and the Hoechst signal using a BP385-470, and a LP560 was used to detect PI. The Zeiss LSM Image Browser was used for image analysis.

TCF promoter activity assay. TF-1 cells were transiently transfected with TOP-5 TCF/LEF-1 reporter plasmid encoding firefly luciferase or the FOP-5 control,[41] and cotransfected with pRL-TK encoding *Renilla* luciferase as an internal control for transfection efficiency. The transfection was performed for 19 hours using Lipofectamine (Invitrogen, San Diego, CA) according to the manufacturer's instructions. After transfection, 10^5 cells were plated in 500 μl RPMI + 2% FBS supplemented with 5 ng/ml granulocyte macrophage–colony-stimulating factor in a 24-well plate, and 500 nmol/l BIO (Calbiochem, San Jose, CA) or 20 mmol/l lithium (Sigma-Aldrich, St. Louis, MO) or 10 μmol/l of peptide constructs. In the latter case, cells were first incubated on ice for 15 minutes in 100 μl Hanks balanced salt solution without calcium or magnesium before addition of 10 μmol/l TAT, eIF2B, or TAT-eIF2B. Cells were then electropulsed at 140 V and resuspended in 500 μl RPMI + 2% FBS + 5 ng/ml granulocyte macrophage–colony-stimulating factor. All samples were incubated at 37 °C for 24 hours, washed with phosphate-buffered saline, and lysed in 100 μl passive lysis buffer. Luciferase activity was measured in 10 μl of cell lysate with a MicroLumat Plus LB 96V Luminometer (Berthold Technologies, Bad Wildbad, Germany) using the Dual Luciferase Assay System (Promega, Madison, WI). After normalizing firefly luciferase activity to that of *Renilla* luciferase, FOP-5 was used to normalize the TOP-5 signal.

SUPPLEMENTARY MATERIAL

Figure S1. The viability of cells exposed to an electrical pulse is dependent on cell type and voltage.

Figure S2. Confocal microscopy images of TF-1 cells treated with TAT-SA-PE (red) at (**a**) 0 V and (**b**) 140 V, and TF-1 cells exposed to TAT-eIF2B (green) at (**c**) 0 V and (**d**) 130 V.

ACKNOWLEDGMENTS

This work was supported by grants from the Canadian Institutes of Health Research and the National Alliance for Research on Schizophrenia And Depression, the World's Leading Charity Dedicated to Mental Health. We are grateful to HC Clevers (University Hospital, Utrecht, the Netherlands) for providing the TOP-5 TCF/LEF-1 reporter plasmid encoding firefly luciferase and Tamara Holowacz (University of Toronto, Canada) for helping with the transfection and the luciferase assay.

REFERENCES

1. Viehl, CT, Becker-Hapak, M, Lewis, JS, Tanaka, Y, Liyanage, UK, Linehan, DC *et al.* (2005). A tat fusion protein-based tumor vaccine for breast cancer. *Ann Surg Oncol* **12**: 517–525.
2. Moy, P, Daikh, Y, Pepinsky, B, Thomas, D, Fawell, S and Barsoum, J (1996). Tat-mediated protein delivery can facilitate MHC class I presentation of antigens. *Mol Biotechnol* **6**: 105–113.
3. Hu, M, Wang, J, Chen, P and Reilly, RM (2006). HIV-1 Tat peptide immunoconjugates differentially sensitize breast cancer cells to selected antiproliferative agents that induce the cyclin-dependent kinase inhibitor p21WAF-1/CIP-1. *Bioconjug Chem* **17**: 1280–1287.
4. Krosl, J, Austin, P, Beslu, N, Kroon, E, Humphries, RK and Sauvageau, G (2003). *In vitro* expansion of hematopoietic stem cells by recombinant TAT-HOXB4 protein. *Nat Med* **9**: 1428–1432.
5. Kwon, YD, Oh, SK, Kim, HS, Ku, SY, Kim, SH, Choi, YM *et al.* (2005). Cellular manipulation of human embryonic stem cells by TAT-PDX1 protein transduction. *Mol Ther* **12**: 28–32.
6. Dominguez-Bendala, J, Klein, D, Ribeiro, M, Ricordi, C, Inverardi, L, Pastori, R *et al.* (2005). TAT-mediated neurogenin 3 protein transduction stimulates pancreatic endocrine differentiation *in vitro*. *Diabetes* **54**: 720–726.
7. Derossi, D, Calvet, S, Trembleau, A, Brunissen, A, Chassaing, G and Prochiantz, A (1996). Cell internalization of the third helix of the Antennapedia homeodomain is receptor-independent. *J Biol Chem* **271**: 18188–18193.
8. Gazit, E, Lee, WJ, Brey, PT and Shai, Y (1994). Mode of action of the antibacterial cecropin B2: a spectrofluorometric study. *Biochemistry* **33**: 10681–10692.
9. Tunnemann, G, Martin, RM, Haupt, S, Patsch, C, Edenhofer, F and Cardoso, MC (2006). Cargo-dependent mode of uptake and bioavailability of TAT-containing proteins and peptides in living cells. *FASEB J* **20**: 1775–1784.
10. Vives, E (2003). Cellular uptake [correction of utake] of the Tat peptide: an endocytosis mechanism following ionic interactions. *J Mol Recognit* **16**: 265–271.
11. Kaplan, IM, Wadia, JS and Dowdy, SF (2005). Cationic TAT peptide transduction domain enters cells by macropinocytosis. *J Control Release* **102**: 247–253.
12. Joliot, A and Prochiantz, A (2008). Homeoproteins as natural Penetratin cargoes with signaling properties. *Adv Drug Deliv Rev* **60**: 608–613.
13. Manceur, A, Wu, A and Audet, J (2007). Flow cytometric screening of cell-penetrating peptides for their uptake into embryonic and adult stem cells. *Anal Biochem* **364**: 51–59.
14. David, G (1993). Integral membrane heparan sulfate proteoglycans. *FASEB J* **7**: 1023–1030.
15. Sandgren, S, Cheng, F and Belting, M (2002). Nuclear targeting of macromolecular polyanions by an HIV-Tat derived peptide. Role for cell-surface proteoglycans. *J Biol Chem* **277**: 38877–38883.
16. Tyagi, M, Rusnati, M, Presta, M and Giacca, M (2001). Internalization of HIV-1 tat requires cell surface heparan sulfate proteoglycans. *J Biol Chem* **276**: 3254–3261.
17. Turner, JJ, Ivanova, GD, Verbeure, B, Williams, D, Arzumanov, AA, Abes, S *et al.* (2005). Cell-penetrating peptide conjugates of peptide nucleic acids (PNA) as inhibitors of HIV-1 Tat-dependent trans-activation in cells. *Nucleic Acids Res* **33**: 6837–6849.
18. Shiraishi, T, Pankratova, S and Nielsen, PE (2005). Calcium ions effectively enhance the effect of antisense peptide nucleic acids conjugated to cationic tat and oligoarginine peptides. *Chem Biol* **12**: 923–929.
19. Abes, S, Williams, D, Prevot, P, Thierry, A, Gait, MJ and Lebleu, B (2006). Endosome trapping limits the efficiency of splicing correction by PNA-oligolysine conjugates. *J Control Release* **110**: 595–604.
20. Shiraishi, T and Nielsen, PE (2006). Photochemically enhanced cellular delivery of cell penetrating peptide-PNA conjugates. *FEBS Lett* **580**: 1451–1456.
21. Wadia, JS, Stan, RV and Dowdy, SF (2004). Transducible TAT-HA fusogenic peptide enhances escape of TAT-fusion proteins after lipid raft macropinocytosis. *Nat Med* **10**: 310–315.
22. Clarke, E, Pereira, C, Chaney, R, Woodside, S, Eaves, AC and Damen, J (2007). Toxicity testing using hematopoietic stem cell assays. *Regen Med* **2**: 947–956.
23. Peng, SB, Yan, L, Xia, X, Watkins, SA, Brooks, HB, Beight, D *et al.* (2005). Kinetic characterization of novel pyrazole TGF-beta receptor I kinase inhibitors and their blockade of the epithelial-mesenchymal transition. *Biochemistry* **44**: 2293–2304.
24. Lakowicz, JR (2006). *Principles of Fluorescence Microscopy*. Springer: New York. 954pp.
25. Weber, PC, Ohlendorf, DH, Wendoloski, JJ and Salemme, FR (1989). Structural origins of high-affinity biotin binding to streptavidin. *Science* **243**: 85–88.
26. Welsh, GI, Patel, JC and Proud, CG (1997). Peptide substrates suitable for assaying glycogen synthase kinase-3 in crude cell extracts. *Anal Biochem* **244**: 16–21.
27. Soughayer, JS, Wang, Y, Li, H, Cheung, SH, Rossi, FM, Stanbridge, EJ *et al.* (2004). Characterization of TAT-mediated transport of detachable kinase substrates. *Biochemistry* **43**: 8528–8540.
28. Bogoyevitch, MA, Barr, RK and Ketterman, AJ (2005). Peptide inhibitors of protein kinases-discovery, characterisation and use. *Biochim Biophys Acta* **1754**: 79–99.
29. Krosl, G, He, G, Lefrancois, M, Charron, F, Romeo, PH, Jolicoeur, P *et al.* (1998). Transcription factor SCL is required for c-kit expression and c-Kit function in hemopoietic cells. *J Exp Med* **188**: 439–450.
30. Birkenkamp, KU, Esselink, MT, Kruijer, W and Vellenga, E (1999). Differential effects of interleukin-3 and interleukin-1 on the proliferation and interleukin-6 protein secretion of acute myeloid leukemic cells; the involvement of ERK, p38 and STAT5. *Eur Cytokine Netw* **10**: 479–490.
31. Tompers, DM and Labosky, PA (2004). Electroporation of murine embryonic stem cells: a step-by-step guide. *Stem Cells* **22**: 243–249.
32. Van Meirvenne, S, Straetman, L, Heirman, C, Dullaers, M, De Greef, C, Van Tendeloo, V *et al.* (2002). Efficient genetic modification of murine dendritic cells by electroporation with mRNA. *Cancer Gene Ther* **9**: 787–797.
33. Oliveira, DM and Goodell, MA (2003). Transient RNA interference in hematopoietic progenitors with functional consequences. *Genesis* **36**: 203–208.
34. Gehl, J (2003). Electroporation: theory and methods, perspectives for drug delivery, gene therapy and research. *Acta Physiol Scand* **177**: 437–447.
35. Antov, Y, Barbul, A and Korenstein, R (2004). Electroendocytosis: stimulation of adsorptive and fluid-phase uptake by pulsed low electric fields. *Exp Cell Res* **297**: 348–362.
36. Antov, Y, Barbul, A, Mantsur, H and Korenstein, R (2005). Electroendocytosis: exposure of cells to pulsed low electric fields enhances adsorption and uptake of macromolecules. *Biophys J* **88**: 2206–2223.
37. Fischer, R, Fotin-Mleczek, M, Hufnagel, H and Brock, R (2005). Break on through to the other side-biophysics and cell biology shed light on cell-penetrating peptides. *Chembiochem* **6**: 2126–2142.
38. Miller, CL, Dykstra, B and Eaves, CJ (2008). Characterization of mouse hematopoietic stem and progenitor cells. *Curr Protoc Immunol* **Chapter 22**: Unit 22B 22.
39. Fok, EY and Zandstra, PW (2005). Shear-controlled single-step mouse embryonic stem cell expansion and embryoid body-based differentiation. *Stem Cells* **23**: 1333–1342.
40. Richard, JP, Melikov, K, Vives, E, Ramos, C, Verbeure, B, Gait, MJ *et al.* (2003). Cell-penetrating peptides. A reevaluation of the mechanism of cellular uptake. *J Biol Chem* **278**: 585–590.
41. Barker, N, van Es, JH, Kuipers, J, Kujala, P, van den Born, M, Cozijnsen, M *et al.* (2007). Identification of stem cells in small intestine and colon by marker gene Lgr5. *Nature* **449**: 1003–1007.